

New insights into the nanostructure of innovative thin film solar cells gained by positron annihilation spectroscopy

Eijt, Stephan; Shi, Wenqin; Mannheim, A.; Butterling, Maik; Schut, Henk; Egger, W; Dickmann, M.; Hugenschmidt, C; Shakeri, B.; Meulenberg, R.W.

DOI

[10.1088/1742-6596/791/1/012021](https://doi.org/10.1088/1742-6596/791/1/012021)

Publication date

2017

Document Version

Final published version

Published in

Journal of Physics: Conference Series

Citation (APA)

Eijt, S., Shi, W., Mannheim, A., Butterling, M., Schut, H., Egger, W., Dickmann, M., Hugenschmidt, C., Shakeri, B., Meulenberg, R. W., Callewaert, V., Saniz, R., Partoens, B., Barbiellini, B., Bansil, A., Melskens, J., Zeman, M., Smets, A., Kulbak, M., ... Brück, E. (2017). New insights into the nanostructure of innovative thin film solar cells gained by positron annihilation spectroscopy. *Journal of Physics: Conference Series*, 791, Article 012021. <https://doi.org/10.1088/1742-6596/791/1/012021>

Important note

To cite this publication, please use the final published version (if applicable).
Please check the document version above.

Copyright

Other than for strictly personal use, it is not permitted to download, forward or distribute the text or part of it, without the consent of the author(s) and/or copyright holder(s), unless the work is under an open content license such as Creative Commons.

Takedown policy

Please contact us and provide details if you believe this document breaches copyrights.
We will remove access to the work immediately and investigate your claim.

New insights into the nanostructure of innovative thin film solar cells gained by positron annihilation spectroscopy

S W H Eijt¹, W Shi¹, A Mannheim¹, M Butterling¹, H Schut¹, W Egger², M Dickmann², C Hugenschmidt³, B Shakeri⁴, R W Meulenberg⁵, V Callewaert⁶, R Saniz⁶, B Partoens⁶, B Barbiellini⁷, A Bansil⁷, J Melskens⁸, M Zeman⁸, A H M Smets⁸, M Kulbak⁹, G Hodes⁹, D Cahen⁹ and E Brück¹

¹ Department of Radiation Science and Technology, Delft University of Technology, NL-2629 JB Delft, Netherlands

² Institut für Angewandte Physik und Messtechnik, Universität der Bundeswehr München, D-85579 Neubiberg, Germany

³ Physik-Department & Heinz Maier-Leibnitz Zentrum (MLZ), Technische Universität München, D-85748 Garching, Germany

⁴ Department of Chemistry, University of Maine, Orono, ME 04469, USA

⁵ Department of Physics and Astronomy and the Laboratory for Surface Science and Technology, University of Maine, Orono ME 04469, USA

⁶ Department of Physics, University of Antwerp, B-2020 Antwerp, Belgium

⁷ Department of Physics, Northeastern University, Boston, MA 02115, USA

⁸ Photovoltaic Materials and Devices, Faculty of Electrical Engineering, Mathematics and Computer Science, Delft University of Technology, NL-2628 CD, Netherlands

⁹ Department of Materials & Interfaces, Weizmann Institute of Science, Rehovot, 76100, Israel

E-mail: s.w.h.eijt@tudelft.nl

Abstract. Recent studies showed that positron annihilation methods can provide key insights into the nanostructure and electronic structure of thin film solar cells. In this study, positron annihilation lifetime spectroscopy (PALS) is applied to investigate CdSe quantum dot (QD) light absorbing layers, providing evidence of positron trapping at the surfaces of the QDs. This enables one to monitor their surface composition and electronic structure. Further, 2D-Angular Correlation of Annihilation Radiation (2D-ACAR) is used to investigate the nanostructure of divacancies in photovoltaic-high-quality a-Si:H films. The collected momentum distributions were converted by Fourier transformation to the direct space representation of the electron-positron autocorrelation function. The evolution of the size of the divacancies as a function of hydrogen dilution during deposition of a-Si:H thin films was examined. Finally, we present a first positron Doppler Broadening of Annihilation Radiation (DBAR) study of the emerging class of highly efficient thin film solar cells based on perovskites.

1. Introduction

Solar cell technology is rapidly developing into one of the main sources of electrical energy. The efficiencies of photovoltaic (PV) devices have reached high values for many types of solar cells [1, 2]; for example, record values of 25.6% and 21.7% for solar cells based on c-Si wafers and Cu(In,Ga)Se₂



thin films, respectively, were reported recently [2]. Solar cells based on a-Si:H and mc-Si:H thin films, which have a high market potential for applications requiring flexible solar cell modules, reached efficiencies of up to 14.0% in triple-junction configurations [3]. Also, new concepts, such as PV devices based on PbS quantum dot (QD) films have currently reached already respectable efficiencies of 10.7% [4]. Furthermore, recent years showed a rather spectacular increase in efficiency for the emerging class of hybrid organic-inorganic perovskite solar cells, with a record of 21.0% reached for a mixture of methyl ammonium lead bromide (MAPbBr₃) and formamidinium lead iodide (FAPbI₃) [5].

In this field, the application of positron annihilation methods for sophisticated thin film analysis is promising, as new insights can be obtained into the presence and types of open volume defects, the local nanostructure and the electronic structure of the various functional layers of thin film PV devices [6-12], and in-situ studies can be envisioned. Moreover, the depth range accessible to low-energy positron beam systems, typically between ~10 nm and several μm s below the surface, matches very well with the thicknesses of a wide range of technologically relevant functional solar cell layers.

In our previous studies, we found that positrons implanted in thin films of PbSe or CdSe QDs have a very high probability to trap at the surfaces of the colloidal QDs. The observed positron-electron momentum distributions can be used to extract information on the composition of their surfaces, gaining new insights into ligand-surface interactions and surface oxidation processes [8, 13]. Furthermore, they provide information about the electronic structure and electronic coupling of CdSe and PbSe QDs [7-10, 13]. Positron annihilation was further applied as one of the main techniques to demonstrate that the nanostructure of hydrogenated amorphous silicon (a-Si:H) is more complex than the conventional model of a Continuous Random Network (CRN) [11, 12]. Instead, open volume deficiencies such as divacancies are present in a CRN-like environment and form a key ingredient to understand the nanostructure and functional properties of a-Si:H solar cell absorber layers. Finally, new insights into the evolution of vacancies in ZnO:Al transparent conductive oxide (TCO) electrodes were obtained upon both fast laser annealing [14] and accelerated environmental degradation [15].

The present paper reports on recent results on advanced characterization of thin film solar cells with positrons. We first provide evidence of trapping of positrons at the surfaces of CdSe QDs using positron annihilation lifetime spectroscopy (PALS). We then apply the 2D-ACAR method to study the nanostructure of divacancies in a-Si:H. The collected momentum distributions are converted by Fourier transformation to a direct space representation given by the electron-positron autocorrelation function $B^{2\gamma}(r)$. The evolution of the nanostructure as a function of hydrogen dilution used in the deposition of a-Si:H was determined, since hydrogen dilution is an important factor influencing the stability against light-induced-degradation. Finally, we present a first positron Doppler broadening study of the emerging class of highly efficient thin film solar cells based on perovskites.

2. Experimental

CdSe QDs with a size of ~4 nm were synthesized according to the methods described in [16, 17] capped with stearic acid and trioctylphosphine oxide ligands. The number density of ligands on the surface of the QD can be systemically tuned by control of the QD cleaning process [17]. The CdSe QDs were drop casted as a thick layer ($> 4 \mu\text{m}$) onto a $10 \times 10 \text{ mm}^2$ sapphire substrate for the PALS study at the PLEPS spectrometer of the NEPOMUC facility. Lifetime spectra consisting of $4 \cdot 10^6$ counts were collected at positron implantation energies in the range of 1-18 keV. The lifetime analysis was performed using both the LT and POSWIN software packages in order to check consistency.

A series of a-Si:H thin films with a thickness of ~450 nm was deposited by Plasma Enhanced Chemical Vapor Deposition on Corning Eagle XG glass substrates, at various hydrogen dilution flow ratios $R = [H_2]/[SiH_4]$ in the range of $R=0$ to $R=10$ [18]. The samples were characterized by Doppler depth-profiling in the range of 0.1-25 keV using the VEP facility. Positron 2D-ACAR distributions were collected using the POSH-ACAR facility at a positron implantation energy of 3.7 keV.

Two perovskite CsPbBr₃ thin films were spin-coated on In-doped tin oxide (ITO) coated glass substrates using the synthesis method described in [19]. Positron Doppler broadening S and W

parameter depth-profiles [11] were collected on the as-deposited films and on the two samples after 3 and 5 months of storage under ambient conditions in the dark. The depth-profiles collected in the range of 0.1–25 keV using the VEP facility were analyzed using the VEPFIT software package [11].

3. Trapping of positrons at the surfaces of CdSe QDs: evidence from lifetime spectroscopy

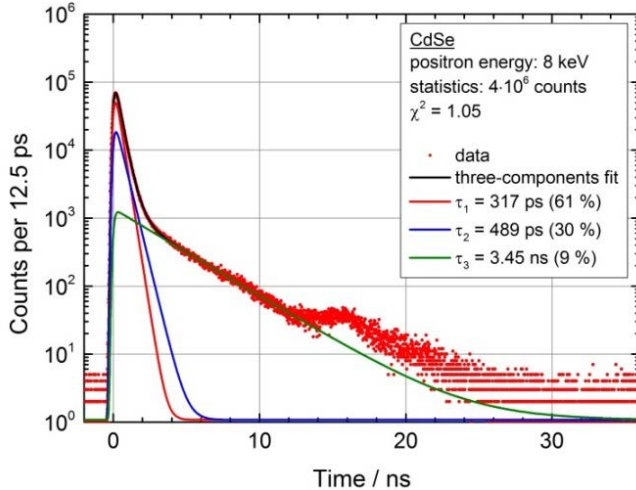


Figure 1. Positron annihilation lifetime spectrum of a thick layer of CdSe QDs deposited on a sapphire substrate, collected at a positron implantation energy of 8 keV. The full lines are the fit curves obtained from a three-lifetime-component analysis.

Previous positron 2D-ACAR studies of CdSe QDs indicated that positrons trap at the local open space present near the surfaces of the QDs, based on the information contained in electron-positron momentum distributions [7]. Here, we present evidence based on positron lifetime spectroscopy that a large fraction of positrons implanted into a thick layer of CdSe QDs indeed annihilate from a trapped state at the surfaces of CdSe QDs, similar to what was previously revealed for PbSe QDs [8].

Figure 1 shows the positron annihilation lifetime spectrum of the CdSe QD layer collected at a positron implantation energy of 8 keV. A three-component lifetime analysis leads to a satisfactory fit. The small bump in the spectrum at ~ 16 ns is due to back-scattering of positrons, and does not affect the three-component analysis. In the range of 4–16 keV, the three-lifetime-component analysis revealed a short lifetime component τ_1 in the range of ~ 320 – 350 ps with a high intensity of $\sim 60\%$ – 85% , and a second (short) lifetime τ_2 in the range of ~ 460 – 550 ps with an intensity of $\sim 30\%$ – 10% . The lifetime of both components likely corresponds to annihilation from positrons trapped at the surfaces of CdSe QDs, where the second lifetime component could be associated with a surface state with less overlap of the positron wave function with electron orbitals. Notably, the average lifetime of the first two components was found to be constant throughout the positron implantation range of 4 keV to 18 keV, with $\tau_{mean} \approx 379 \pm 5$ ps and an intensity of $92 \pm 1\%$, *i.e.* quite close to the values obtained in our previous positron studies on PbSe QD layers [8]. The positron lifetime is much larger than that of defect-free CdSe (275 ps [9]) and, combined with its high intensity, provides strong support for trapping and annihilation of positrons at the surfaces of the CdSe QDs, consistent with previous 2D-ACAR studies [7, 10]. The preliminary outcome of our ab-initio calculations on CdSe slabs using the Local Density Approximation and a Corrugated-Image-Potential indicates that the positron density peaks just below the CdSe surface, while preliminary calculations using the Weighted Density Approximation point to the presence of a true positron surface state.

The third, long lifetime component with $\tau_3 \sim 3.5 \pm 0.1$ ns and $I_3 = 8 \pm 1\%$ corresponds to pick-off annihilation of o-Ps formed in the available open space in between the ligands at the surfaces of the CdSe QDs. The lifetime of this o-Ps component is larger than the values of ~ 2.0 – 2.7 ns for PbSe QDs capped with oleic acid ligands [8]. This finding infers a somewhat larger open space of ~ 0.8 nm in diameter for the case of CdSe QDs with stearic acid and TOPO ligands compared to ~ 0.65 nm for PbSe QDs with oleic acid ligands, as deduced from the Tao-Eldrup model [20].

4. Size evolution of small vacancy clusters in hydrogenated amorphous silicon: 2D-ACAR study

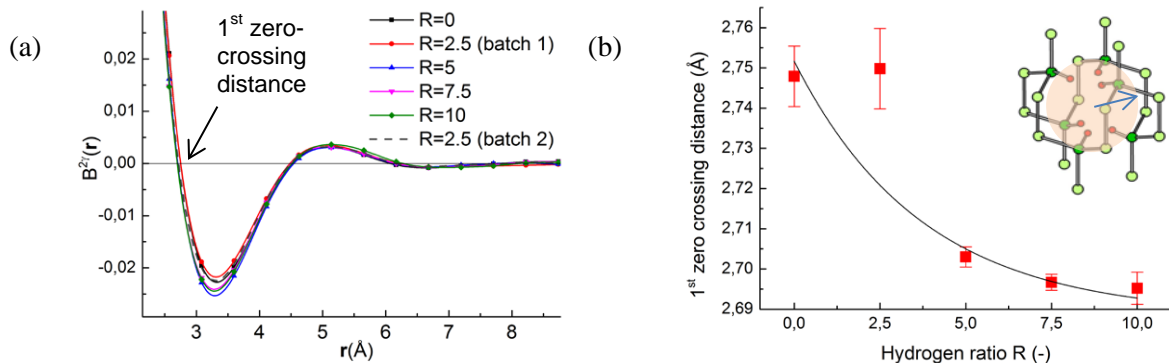


Figure 2. (a) Electron-positron autocorrelation function $B^{2\gamma}(r)$ for as-deposited a-Si:H as a function of hydrogen dilution ratio R . (b) First zero-crossing distance as a function of R . The line is a guide-to-the-eye. The inset is a schematic representation of a Si-divacancy decorated with 6 hydrogen atoms.

In Figure 2(a), we present the electron-positron autocorrelation function $B^{2\gamma}(r)$ as a function of hydrogen dilution ratio R , in order to examine the evolution in the size of open volume deficiencies in a-Si:H films on hydrogen concentration. For each sample, the autocorrelation function was extracted from the collected isotropic 2D-ACAR momentum distribution, using a Fourier transformation of the corresponding 1D-ACAR distribution $N(p)$ [21, 22]. $B^{2\gamma}(r)$ represents the real space autocorrelation function of the electron orbitals modulated by the wave function of the positron, and can thus provide insights into the local spatial environment of the positron annihilation site. In particular, the first zero-crossing in the autocorrelation function provides an indication of the shortest average distance, in any direction, to the site which cannot be occupied by a positron [23]. This can be understood since this distance corresponds to the distance of the center of the positron annihilation site to a nearest neighbour atomic site where the positron wave function $\psi_+(\vec{r})$ necessarily vanishes.

In Figure 2(b), we present the extracted first zero-crossing distances as a function of hydrogen dilution ratio R . The observed first zero-crossing distances of ~ 2.75 Å provide additional support to the picture that the dominant open volume deficiencies in high-quality a-Si:H films are small vacancies (in particular divacancies), as previously proposed based on Doppler broadening S parameter measurements and Fourier transform infrared spectroscopy [11, 12]. Namely, the distance of the center of the positron wave function in an unrelaxed divacancy (in c-Si) to one of the six nearest neighbour Si positions is 2.96 Å, while the corresponding distance of 2.35 Å for an unrelaxed monovacancy is much shorter. The observed first zero-crossing distance of ~ 2.75 Å indicates a local inward relaxation of the Si atom positions around the divacancy, as could be expected [24]. Furthermore, the presence of up to six hydrogen atoms decorating the nearest neighbour Si atoms will also reduce the locally available open space. With increased hydrogen dilution ratio, the first zero crossing is seen to move towards smaller distances of ~ 2.70 Å, correlating with the observed reduction in S parameter for the same set of films. The decrease in the first zero-crossing distance corresponds to $\sim 5\%$ reduction in open volume, and can be caused by additional hydrogen locally present near the boundary of the divacancy. Figure 2(a) moreover shows that the first minimum in $B^{2\gamma}(r)$ at ~ 3.25 Å becomes more pronounced with an increase in R , as the smaller open space induces a larger overlap between the positron wave function and electron orbitals, and thus, a stronger spatial correlation of the positron and electrons. In short, the 2D-ACAR studies provide additional support for the presence of small open volume deficiencies (in particular divacancies) in a CRN environment in a-Si:H films. With increased hydrogen dilution, more hydrogen is present in the close vicinity of the divacancy, effectively reducing the open space available to the positron.

5. Doppler broadening depth profiling study of CsPbBr₃ perovskite solar cell films

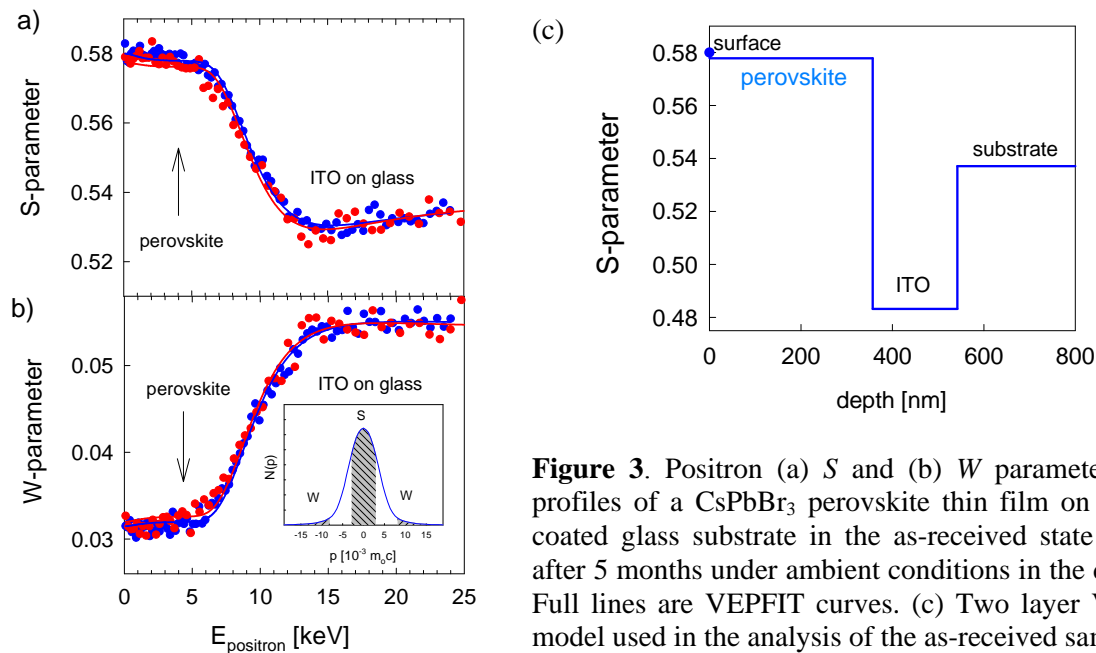


Figure 3. Positron (a) S and (b) W parameter depth profiles of a CsPbBr₃ perovskite thin film on an ITO coated glass substrate in the as-received state (•) and after 5 months under ambient conditions in the dark (•). Full lines are VEPFIT curves. (c) Two layer VEPFIT model used in the analysis of the as-received sample.

Finally, CsPbBr₃ perovskite thin films were studied, since the role of point defects in the degradation mechanism of the emerging class of perovskite solar cells is a topic of debate [25], and, furthermore, vacancies may form unwanted recombination centres for charge carriers [2], limiting the open circuit voltages and solar cell efficiencies reached in practice.

Figure 3 shows the Doppler depth-profiles of one of the CsPbBr₃ thin films on an ITO coated substrate in the as-received state and in the final state after 5 months of exposure to ambient conditions in the dark. The changes in depth-profiles are very small for both samples, as the change in the fit values for S and W for the perovskite layer is only $\Delta S/S_0 \sim -0.3 \pm 0.1\%$ and $\Delta W/W \sim 1 \pm 1\%$, respectively. It is instructive to compare these modest changes to typical values for the shift in S and W upon formation of cation monovacancies. For example, saturation trapping in Zn monovacancies in c -ZnO leads to substantially larger shifts of $\Delta S/S_{c-ZnO} \sim +5.5\%$ and $\Delta W/W_{c-ZnO} \sim -19\%$ [26, 27]. Furthermore, the sign of the small change in S for CsPbBr₃ is opposite. Doppler broadening spectroscopy thus indicates that (negatively charged or neutral) V_{Cs} or V_{Pb} cation vacancies are not visibly generated during prolonged exposure of CsPbBr₃ to ambient conditions in the dark. CsPbBr₃ perovskite solar cells are substantially more stable against environmental degradation than the methyl ammonium lead bromide (MAPbBr₃) based solar cells [19]. Therefore, positron depth profiling studies of MAPbBr₃, including also degradation under AM1.5 solar illumination conditions [19], seem promising in order to unravel whether or not the formation of cation vacancies is a key element in the degradation of perovskite-based solar cells [25]. It should be noted that, since V_{Br} monovacancies mostly are positively charged, positrons are not expected to trap in the anion vacancies, and are largely insensitive to the presence of such monovacancies. Therefore, the formation of V_{Br} monovacancies cannot be excluded for the CsPbBr₃ films investigated in this study.

6. Conclusions

PALS has revealed that a high fraction of positrons implanted in CdSe QD films trap at the surfaces of the QDs. Depth-profiling positron methods show high potential as a characterization tool for the surface composition and electronic structure of colloidal semiconductor QDs embedded as the functional layer of innovative PV devices. Positron methods can aid the development of such QD-

based PV devices, since present limitations in their solar cell efficiency involve surface recombination of generated charge carriers and inefficient transport of charge carriers involving hopping conductivity, requiring optimization of surface passivation and electronic coupling between neighbouring QDs as well as a reduction of transport barriers. These factors form key contributions to the relatively high loss in open circuit voltage in PV devices, and tailoring of the surface properties and electronic coupling of QDs may lead to further large improvements in solar cell efficiencies.

Further, 2D-ACAR was used to examine the evolution of the size of divacancies in a-Si:H films as a function of hydrogen dilution during synthesis. Such open volume deficiencies form a key ingredient to understand and tailor the nanostructure of a-Si:H films, which may aid the development of synthesis procedures to stabilize a-Si:H absorber layers against light induced degradation.

Finally, positron Doppler depth-profiling was applied to examine the relatively high stability of CsPbBr₃ perovskite solar cells. Exposure to ambient conditions in the dark for 5 months did not lead to visible formation of cation vacancies.

Acknowledgments

The work at Delft University of Technology was supported by the China Scholarship Council (CSC) grant of W.S., by ADEM, A green Deal in Energy Materials of the Ministry of Economic Affairs of The Netherlands (www.adem-innovationlab.nl), and the STW Vidi grant of A.S., Grant No. 10782. The PALS study is based upon experiments performed at the PLEPS instrument of the NEPOMUC facility at the Heinz Maier-Leibnitz Zentrum (MLZ), Garching, Germany, and was supported by the European Commission under the 7th Framework Programme, Key Action: Strengthening the European Research Area, Research Infrastructures, Contract No. 226507, NMI3. The work at University of Maine was supported by the National Science Foundation under Grant No. DMR-1206940. Research at the University of Antwerp was supported by FWO grants G022414N and G015013. The work at Northeastern University was supported by the US Department of Energy (DOE), Office of Science, Basic Energy Sciences grant number DE-FG02-07ER46352 (core research), and benefited from Northeastern University's Advanced Scientific Computation Center (ASCC), the NERSC supercomputing center through DOE grant number DE-AC02-05CH11231, and support (applications to layered materials) from the DOE EFRC: Center for the Computational Design of Functional Layered Materials (CCDM) under DE-SC0012575. The work at the Weizmann Institute was supported by the Sidney E. Frank Foundation through the Israel Science Foundation, by the Israel Ministry of Science, and the Israel National Nano-Initiative. D.C. holds the Sylvia and Rowland Schaefer Chair in Energy Research.

References

- [1] Nayak P K, Bisquert J and Cahen D 2011 *Adv. Mater.* **23** 2870
- [2] Polman A, Knight M, Garnett E C, Ehrler B and Sinke W 2016 *Science* **352** aad4424
- [3] Sai H, Matsui T and Matsubara K 2016 *Appl. Phys. Lett.* **109** 183506
- [4] Kim G-H *et al.* 2015 *Nano Lett.* **15** 7691
- [5] Brittan S, Adhyaksa G W P, and Garnett E C 2015 *MRS Communications* **5** 7
- [6] Tuomisto F and Makkonen I 2013 *Rev. Mod. Phys.* **85** 1583
- [7] Eijt S W H, van Veen A, Schut H, Mijnaerends P E, Denison A B, Barbiellini B, Bansil A 2006 *Nature Mater.* **5** 23
- [8] Chai L *et al.* 2013 *APL Materials* **1** 022111
- [9] Weber M H, Lynn K G, Barbiellini B, Sterne P A and Denison A B 2002 *Phys. Rev. B* **66** 041305(R)
- [10] Eijt S W H, Mijnaerends P E, van Schaarenburg L C, Houtepen A J, Vanmaekelbergh D, Barbiellini B and Bansil A 2009 *Appl. Phys. Lett.* **94** 091908
- [11] Melskens J, Smets A H M, Schouten M, Eijt S W H, Schut H and Zeman M 2013 *IEEE J. of Photovoltaics* **3** 65
- [12] Melskens J *et al.* 2015 *Phys. Rev. B* **91** 245207
- [13] Shi W, Eijt S W H, Suchand Sandeep C S, Siebbeles L D A, Houtepen A J, Kinge S, Brück E, Barbiellini B and Bansil A 2016 *Appl. Phys. Lett.* **108** 081602
- [14] Scorticati D *et al.* 2015 *Acta Mater.* **98**, 327
- [15] Shi W *et al.*, in preparation
- [16] Lee J R I, Whitley H D, Meulenberg R W *et al.*, 2012 *Nano Lett.* **12** 2763
- [17] Shakeri B and Meulenberg R W 2015 *Langmuir* **31** 13433
- [18] Melskens J, PhD thesis, Delft University of Technology (2015)
- [19] Kulbak M, Gupta S, Kedem N, Levine I, Bendikov T, Hodes G and Cahen D 2016 *J. Phys. Chem. Lett.* **7** 167
- [20] Gidley D W, Peng H-G and Vallery R S 2006 *Annu. Rev. Mater.* **36** 49
- [21] Ho K F, Ching H M, Beling C D, Fung S, Ng K P, Biasini M, Ferro G and Gong M 2003 *J. Appl. Phys.* **94** 5549
- [22] Kobayashi T 2001 *Mater. Sci. Tech.* **363-365** 689
- [23] Britton D T, Minani E, Knoesen D, Schut H, Eijt S W H, Furlan F, Giles C, Härting M 2006 *Appl. Surf. Sci.* **252** 3194
- [24] Makkonen I and Puska M J 2007 *Phys. Rev. B* **76** 054119
- [25] Miller J L 2014 *Physics Today* **67** 13, and Refs. therein
- [26] Kahn E H, Weber M H and McCluskey M D 2013 *Phys. Rev. Lett.* **111** 017401
- [27] Makkonen I, Korhonen E, Prozheeva V and Tuomisto F 2016 *J. Phys.: Condens. Matter.* **28** 224002